Vacuum 168 (2019) 108802

Contents lists available at ScienceDirect

Vacuum

journal homepage: www.elsevier.com/locate/vacuum

Effects of superimposed dual-frequency (13.56/2 MHz) inductively coupled plasma source on the uniformity of Ar/CF_4 plasma

Kyung Chae Yang[a], Ye Ji Shin[a], Hyun Woo Tak[a], Wonseok Lee[b], Seung Bae Lee[b], Geun Young Yeom[a,*]

[a] School of Advanced Materials Science and Engineering, Sungkyunkwan University, Suwon, South Korea
[b] SEMES CO., LTD., 77, 4 Sandan 5-gil, Jiksan-eup, Seobuk-gu, Cheonan, South Korea

ARTICLE INFO

Keywords:
plasma uniformity
Etch uniformity
Inductively coupled plasma
Superimposed dual-frequency

ABSTRACT

As one of the methods for controlling the plasma uniformity, superimposed dual frequencies of 13.56 and 2 MHz were used on an inductively coupled plasma (ICP) source, and the effects of the superimposed dual-frequency ICP on the plasma and etch uniformities were investigated and compared with a conventional single-frequency ICP operation at 13.56 MHz using Ar/CF_4. The superimposed dual-frequency ICP operated at 13.56 and 2 MHz improved the plasma uniformity compared to the single-frequency ICP for both Ar and Ar/CF_4 by improving the plasma density near the center region of the wafer close to the edge region. In addition, for Ar plasma, a change in the power ratio of 2/13.56 MHz during the superimposed dual-frequency operation changed the EEDF of the plasma and the IED toward the wall. When SiO_2 was etched using Ar/CF_4 with the superimposed dual-frequency ICP while biasing the substrate with a separate radio frequency power of 12.56 MHz, similar to the results on the plasma uniformity, the SiO_2 etch uniformity within a 300 mm diameter wafer was improved by using the superimposed dual-frequency ICP operated at 13.56 and 2 MHz, as compared to that using a single-frequency ICP of 13.56 MHz.

1. Introduction

Some of the important specifications for next-generation plasma etch systems are the ultra-high etch selectivity and extremely high uniformity control on the substrate [1]. Particularly for inductively coupled plasma (ICP) sources, as the power to the ICP sources is increased for an increased plasma density, non-uniform power deposition applied to the plasma, resulting in a non-uniformity of the plasma, is increased [2–4]. These days, ICP systems are dominant tools used in industry for plasma etching, with the exception of the etching of SiO_2 with a high aspect ratio, which mostly requires very high energy ions and a very high etch selectivity of SiO_2 to hard mask layers [5–8].

Although ICP sources exhibit significant merits in terms of plasma processing, scaling the plasma sources to larger substrate sizes tends to show problems in the uniformity during plasma processing for the semiconductor and display industries. These are heavily related with the antenna standing wave and skin effects, particularly when the size of the plasma sources is comparable to the wavelength of the driving frequency in the plasma [9–11]. To process a large-area substrate in a uniform manner, precise control of the distribution of the plasma species while biasing the substrate with additional radio frequency (RF) bias power is one of the most significant challenges to the industrial plasma etch processing [12–14]. In particular, the spatial distributions of charged particle densities, the electron and ion temperatures, and voltages near the wafer surface have significant influences on the non-uniform etch characteristics, and which are related to the specific discharge conditions [15–17].

In general, for a typical ICP system, owing to the specific configuration of the antenna, it is difficult to obtain a uniform distribution of the plasma over the substrate surface area in either the radial or azimuthal direction [13,18,19]. To overcome the limitations of plasma and etch non-uniformity for an ICP source, advanced strategies are applied, including the use of a specially shaped electrode [2,12,20–23], the installation of two or more separate ICP antennas with the power split or multiple RF frequencies [24–26], the supply of asymmetric gas pumping [27], or the application of RF power pulsing [28,29]. However, even with these methods, the controllability of the plasma uniformity over a large area remains a major challenge.

In this study, as one of the methods for controlling the plasma uniformity, superimposed dual-frequency operation on an ICP source was investigated. A dual frequency power of 2 and 13.56 MHz was applied to the same ICP antenna, and a bias voltage with a single

* Corresponding author.
E-mail address: gyyeom@skku.edu (G.Y. Yeom).

https://doi.org/10.1016/j.vacuum.2019.108802
Received 16 April 2019; Received in revised form 30 June 2019; Accepted 4 July 2019
Available online 04 July 2019
0042-207X/

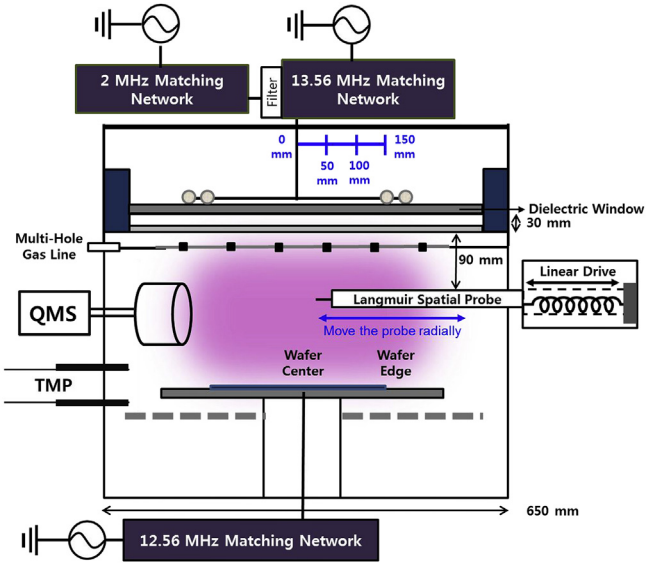

Fig. 1. Schematic diagram of a superimposed dual-frequency ICP etch system with a single Langmuir probe and QMS.

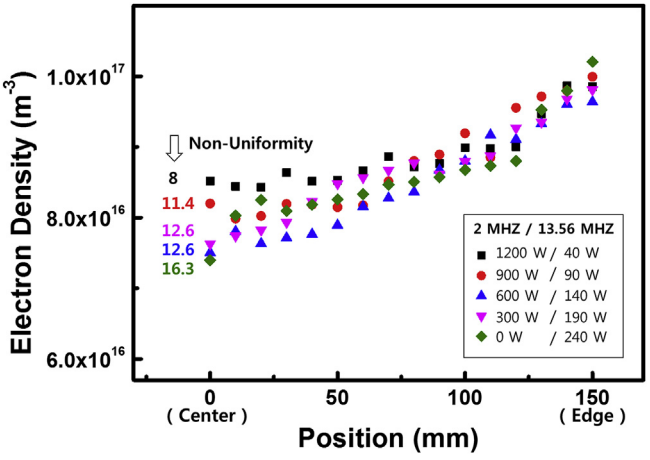

Fig. 2. Electron density for Ar plasmas measured from the center to the edge along the centerline of a 300 mm diameter wafer for different combinations of superimposed dual-frequency ICP powers of 2 MHz (0–1200 W) and 13.56 MHz (40–240 W) RF power. RF powers of 2 and 13.56 MHz were adjusted to obtain similar electron densities at the edge of the wafer. In addition, 20 mTorr, Ar (150 sccm) was used as the operating gas condition.

frequency of 12.56 MHz was applied to the substrate to provide additional improved variables for controlling the plasma parameters. To examine the role of applying superimposed dual frequencies to the ICP on the effect of the uniformity, the plasma characteristics from both single-frequency ICP and superimposed dual-frequency ICP were compared. In addition, the effects of the superimposed dual-frequency ICP on the SiO_2 etch uniformity using Ar/CF_4 were also investigated and compared with those of the single-frequency ICP.

2. Experimental details

A schematic of the ICP plasma reactor (anodized aluminum with 650 mm inner diameter) with a superimposed dual-frequency ICP source is shown in Fig. 1. The ICP antenna applied was a two-turn silver-coated Cu coil with a width of 10 mm and a thickness of 5 mm (inner coil diameter ~380 mm and outer coil diameter ~450 mm). RF powers of 13.56 MHz (SEREN, R10001) and 2 MHz (MKS, NOVA-50 A) were supplied to the same ICP antenna (designed for an operation at

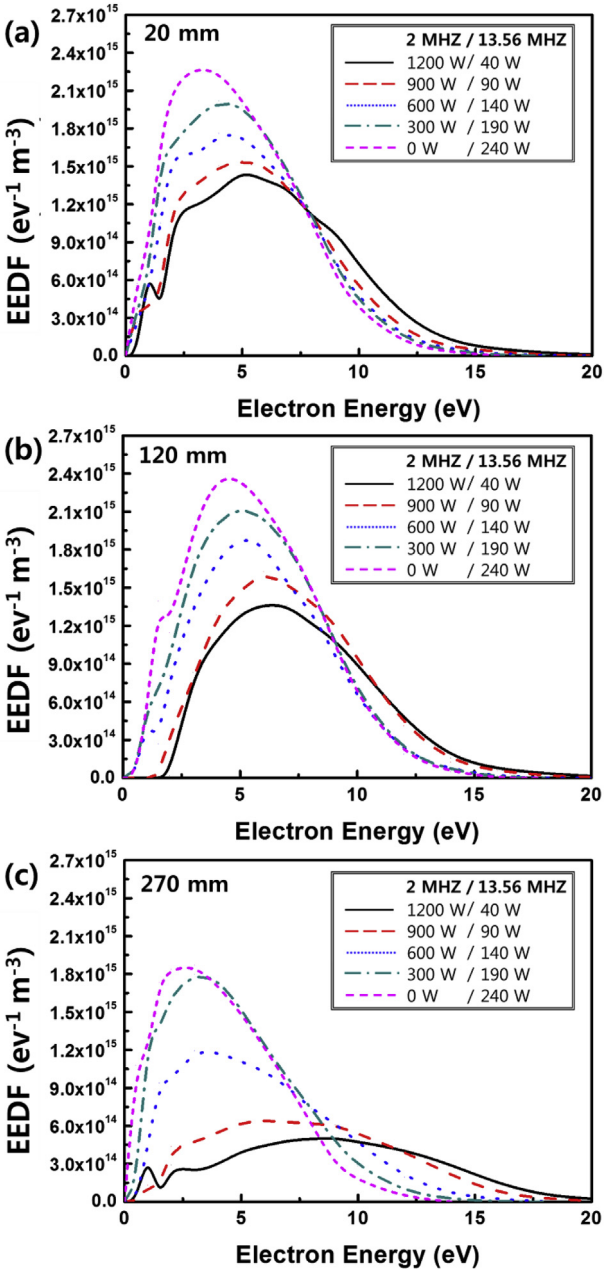

Fig. 3. EEDFs of Ar plasma at different locations for the superimposed dual-frequency ICP for the conditions shown in Fig. 2. 20 mTorr, Ar (150 sccm) was used as the operating gas condition.

13.56 MHz) for sustaining the plasma, and an RF power of 12.56 MHz was used on the bottom electrode for the substrate biasing. The chamber walls are electrically grounded. The L-type matching boxes for both frequencies were modified with a low-pass filter for superimposing the dual-frequency power system. The diameter of the substrate holder was 450 mm. The processing gas was injected through 1 mm diameter holes located beneath the dielectric window and along the cylindrical anodized aluminum chamber wall.

An Ar/CF_4 (150/75 sccm) mixture, or Ar (150 sccm) alone, was used as the discharge gas, and a total pressure of 20 mTorr was maintained using an automatic pressure controller. The low (2 MHz) and high (13.56 MHz) frequency source powers were varied from zero to 1,600, and zero to 800 W, respectively.

A single automated Langmuir probe (ALP-150, Impedance) located at 90 mm below the ICP antenna was used to obtain the spatial profiles

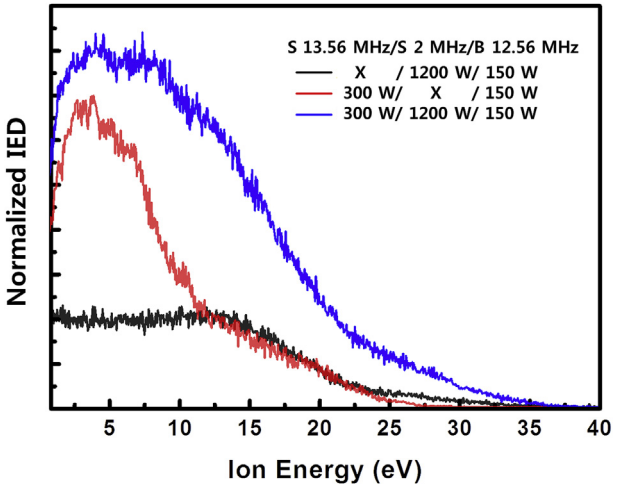

Fig. 4. IEDs of Ar^+ ions measured using the QMS located at the chamber wall for the superimposed dual-frequency ICP composed of 13.56/2 MHz ((300/1200 W) and for the single-frequency ICP of 13.56 MHz (300 W) and 2 MHz (1200 W) only while biasing the substrate at 150 W with 12.56 MHz 20 mTorr, Ar (150 sccm) was used as the operating gas condition.

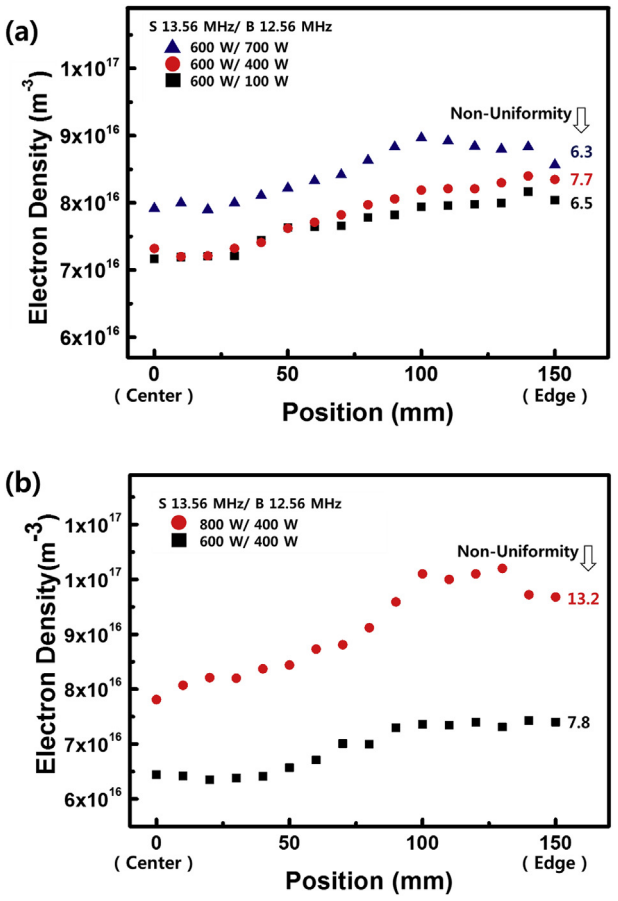

Fig. 5. Spatial distribution of electron density measured (a) as a function of substrate bias power (100–700 W) of 12.56 MHz while operating the ICP source at a single frequency of 13.56 MHz (600 W), and (b) as a function of a single frequency power of 13.56 MHz (600–800 W) to the ICP source while biasing the substrate at 400 W with 12.56 MHz 20 mTorr of Ar/CF_4 (150 sccm/75 sccm) was used as the reactive gas mixture.

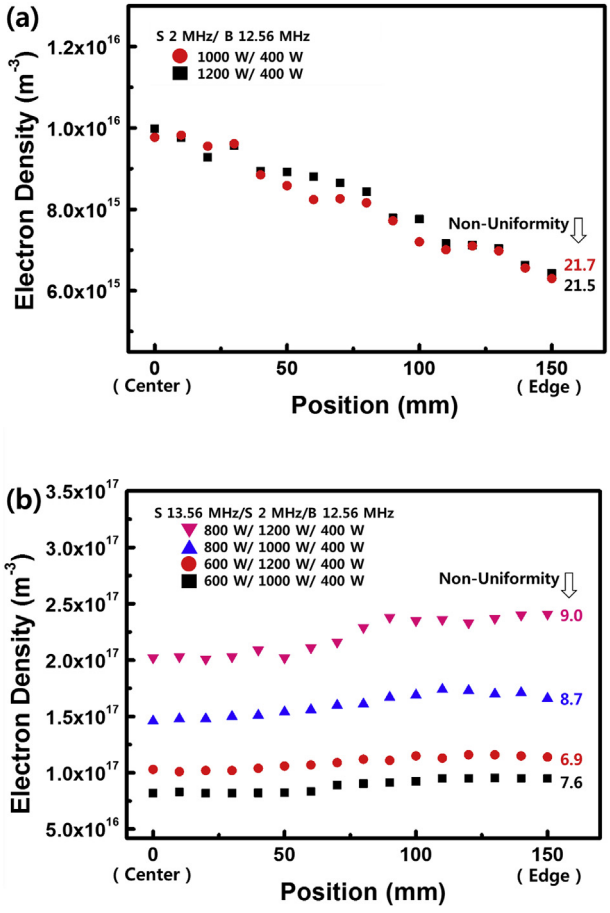

Fig. 6. Spatial distribution of electron density measured (a) as a function of a single-frequency power of 2 MHz (1000–1200 W) to the ICP source, and (b) as a function of superimposed dual-frequency powers of 13.56 MHz (600–800 W) and 2 MHz (1000–1200 W) while biasing the substrate at 400 W with 12.56 MHz 20 mTorr of Ar/CF_4 (150/75 sccm) was used as the reactive gas mixture.

of the plasma parameters, such as electron density and electron energy distribution function (EEDF). The probe's tip was made of tungsten, 0.4 mm in diameter and 10 mm in length. The probe was connected to an extensible bellow and a linear drive to measure the plasma parameters across a 300-mm diameter wafer from the center to the edge at intervals of 10 mm. An RF compensator set for the frequency range compensation of 1–100 MHz was used for a broadband compensation. For the Ar plasma, the ion energy distribution (IED) to the wall was measured using a quadrupole mass spectrometer (QMS, PSM003, Hiden Analytical) with an energy resolution of 0.05 eV. The mass spectrometer was operated in the positive ion detection mode.

For the superimposed dual-frequency ICP condition, 15 SiO_2 coupon (2 cm × 2 cm) samples were distributed in a 300-mm wafer from the edge to the center, both axially and radially, and these SiO_2 coupon samples were etched using an Ar/CF_4 (150/75 sccm) mixture to estimate the etch uniformity. The SiO_2 etch rates were measured using ellipsometry (SE MG-1000 UV). The non-uniformities of the SiO_2 etching and plasma density for the Langmuir probe measurement described above were calculated using the following [16]:

$$Non-uniformity\ (\%) = \frac{(maximum\ value - minimum\ value)}{2 \times average} \quad (1)$$

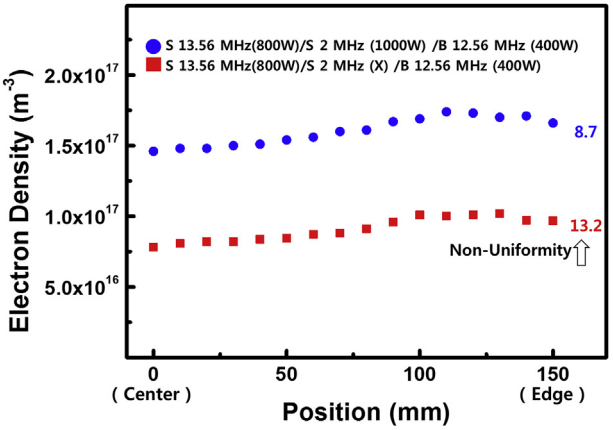

Fig. 7. A comparison of the electron density distribution for a superimposed dual-frequency ICP condition of 13.56 MHz (800 W) and 2 MHz (1000 W), and a single-frequency ICP condition of 13.56 MHz (800 W) while biasing the substrate at 400 W at 12.56 MHz 20 mTorr of Ar/CF_4 (150/75 sccm) was used as the reactive gas mixture.

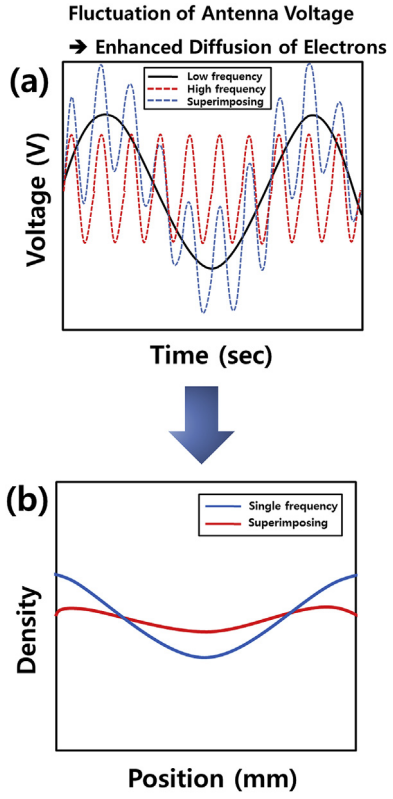

Fig. 8. A cartoon describing a possible mechanism for an improvement of the plasma uniformity using the superimposed dual-frequency ICP: (a) complicated voltages developed on the two-turn ICP antenna and (b) uniformity improvement through the electric field drift of electrons towards radial direction of the wafer by (a).

3. Results and discussion

3.1. Superimposed dual-frequency Ar ICP

The plasma density distributions in the Ar plasmas were investigated for different combinations of RF powers of 2 and 13.56 MHz applied to the superimposed dual-frequency ICP source, the results of which are shown in Fig. 2 for electron density (instead of ion densities, for the comparison with plasma densities of CF_4 plasmas, electron densities were measured.) Here, 20 mTorr, Ar (150 sccm) was used and RF powers of 2 MHz (0–1200 W) and 13.56 MHz (40–240 W) were adjusted to obtain similar electron densities at the edge of the wafer. The electron densities were measured at a distance of 10 mm along the radical position. As shown in Fig. 2, the electron density profiles of Ar plasmas were similar each other, and the electron densities were higher for the edge of the wafer, possibly owing to the higher induced time-varying magnetic and electric fields near the ICP coil compared to the center of the chamber. Therefore, when only 240 W was applied to the ICP antenna at 13.56 MHz, the electron densities at the center of the chamber were the lowest as $\sim 7.4 \times 10^{16}\ m^{-3}$ and the electron densities were increased with an increase in the radius, and, at the edge of a wafer of ~150 mm, $\sim 1 \times 10^{17}\ m^{-3}$ was obtained, resulting in ~16.3% plasma non-uniformity. For the superimposed dual-frequency ICP, the 13.56 MHz RF power was decreased by 40 W, and to maintain a similar plasma density at the edge of the wafer, 2 MHz RF power was added to the same ICP coil through a filter by 300 W (owing to the difficulty in power matching through an ICP antenna of the same length, a higher power was required for 2 MHz RF power), and, as shown in Fig. 2, the electron densities near the center of the wafer were increased with an increased portion of the 2 MHz RF power, and, for 1200 W at 2 MHz and 40 W at 13.56 MHz, a plasma non-uniformity of ~8% could be observed.

The EEDFs of the Ar plasmas used for the superimposed dual-frequency ICP source were measured at different locations along the centerline of the wafer for the plasma conditions shown in Fig. 2, and the results are indicated in Fig. 3(a), (b), and (c) for 20, 120, and 270 mm from the center of the wafer, respectively. As shown in Fig. 3, for the locations within the antenna diameter (20 and 120 mm), the EEDFs were similar for each superimposed dual-frequency ICP condition; however, at the location outside of the ICP antenna (270 mm), the EEDFs were different from those observed within the antenna diameter, possibly owing to the electric field developed near the chamber wall position (that is, a non-plasma region). In addition, the EEDF moved to higher electron energy for the higher 2/13.56 MHz RF power ratio at all locations, particularly at the outside of the antenna diameter (270 mm).

An Ar^+ IED was measured using the QMS located at the chamber wall for a superimposed dual-frequency ICP operated at 13.56 MHz (300 W) and 2 MHz (1200 W), in addition to the Ar^+ IEDs measured for the single-frequency ICP of 13.56 MHz (300 W) and 2 MHz (1200 W) only, and their results are shown in Fig. 4. Here, 20 mTorr Ar (150 sccm) was used as the operating gas condition, and the substrate was biased at 150 W with 12.56 MHz. As shown in Fig. 4, when a single-frequency 2 MHz RF power was used in the ICP antenna, an IED with the average energy of 11 eV and an energy tail of up to 35 eV was observed, however, when a single-frequency 13.56 MHz RF power was used for the ICP antenna, an IED lower than that at 2 MHz was observed with an average energy level of 7 eV and an energy tail reaching 27 eV. The higher ion energy for 2 MHz is thought to be related to the higher energy EEDF, as observed for the higher 2/13.56 MHz power ratio. When the superimposed dual frequencies were applied to the ICP antenna, an IED similar to the combined IED shapes by both 2 and 13.56 MHz could be observed with an average energy level of 10 eV and an energy tail of up to 37 eV.

3.2. Single/superimposed dual-frequency ICP for Ar/CF_4

For the etching of various semiconductor materials, reactive gas mixtures are generally used instead of Ar only, and the substrate is biased with a separate RF power; therefore, using a reactive gas composed of Ar/CF_4, the plasma characteristics of the superimposed dual-frequency ICP were investigated and compared with those of a conventional single-frequency ICP while biasing the substrate. Fig. 5 shows the electron density measured along the centerline of the 300-mm diameter wafer from the center to the edge using a Langmuir probe for the ICP source operated at 13.56 MHz RF power using only 20 mTorr of

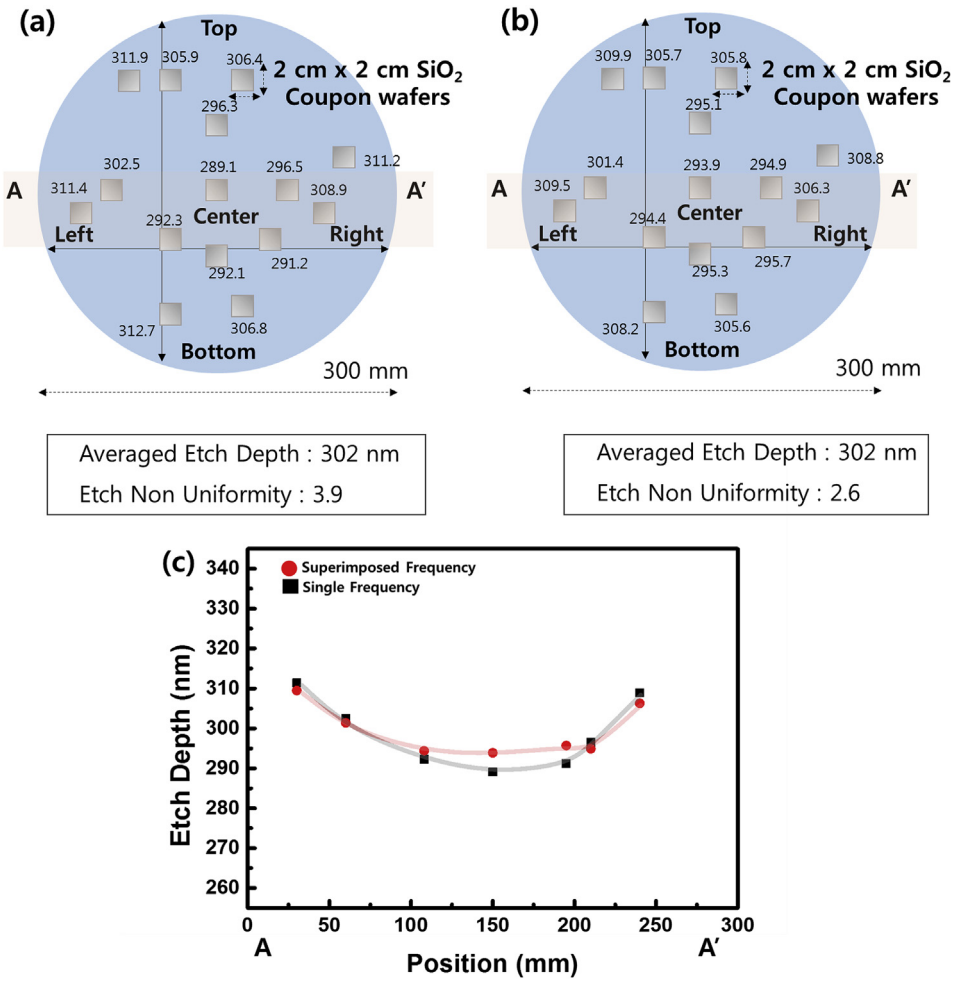

Fig. 9. SiO_2 etch depths for (a) single-frequency ICP operation with 800 W at 13.56 MHz and (b) superimposed dual-frequency ICP operation with 800 W at 13.56 MHz, and 1200 W at 2 MHz, while biasing the substrate with 400 W at 12.56 MHz. For each condition, 15 coupon samples of 2 cm × 2 cm SiO_2 on silicon were used, and for a similar etch amount, the etch time was 4.5 min for a single-frequency 800 W 13.56 MHz ICP, and 3 min for a superimposed dual-frequency ICP operated using 800 W at 13.56 MHz, and 1200 W at 2 MHz. 20 mTorr of Ar/CF_4 (150/75 sccm) was used, and the substrate was biased using a separate RF power of 400 W at 12.56 MHz. (c) etch rates of SiO_2 measured along the 300 mm diameter wafer centerline zone of A-A′ in Fig. 9(a) and (b). (For interpretation of the references to colour in this figure legend, the reader is referred to the Web version of this article.)

the reactive gas combination of Ar/CF_4 (150/75 sccm) while biasing the substrate. Owing to the use of a molecular gas mixture, the electron density measured using the Langmuir probe was also used as the spatial distribution of the plasma density. Fig. 5(a) shows the electron density distribution measured as a function of a substrate bias power (100–700 W) of 12.56 MHz while operating the ICP source at a single frequency of 13.56 MHz (600 W). As shown in Fig. 5(a), the increase in 12.56 MHz RF power from 100 to 700 W increased the plasma density slightly without significantly changing the plasma uniformity because of the low power deposition possibly as a capacitively coupled plasma (CCP), as compared to that of ICP. Fig. 5(b) shows the electron density measured as a function of a single-frequency power of 13.56 MHz (600–800 W) to the ICP source while biasing the substrate at 400 W with 12.56 MHz. The slight increase in 13.56 MHz RF power to the ICP antenna from 600 to 800 W significantly increased the plasma density; however, owing to the non-uniform power deposition along the radial direction by the ICP antenna, the plasma non-uniformity was increased from 7.8% to 13.2% as the 13.56 MHz ICP power was increased from 600 to 800 W, while biasing the substrate at 400 W.

Using 2 MHz RF power instead of 13.56 MHz RF power, the spatial distribution of the electron density for the ICP source operated with a single-frequency power of 2 MHz was also measured while biasing the substrate with 400 W at 12.56 MHz, the result of which is shown in Fig. 6(a). Owing to the insufficient power matching to the ICP antenna with only 2 MHz RF power (2 MHz RF power was matched to the ICP antenna only when it was used along with 13.56 MHz as the superimposed dual-frequency power condition), a low electron density was observed even with the substrate biasing at 400 W of 12.56 MHz. However, different from the spatial distribution of the electron density for 13.56 MHz RF power only, the electron density at the center was higher, whereas at the edge of the wafer, it was lower.

Using a superimposed dual-frequency ICP power composed of 13.56 MHz (600–800 W) and 2 MHz (1000–1200 W), the spatial distribution of the electron density was measured while biasing the substrate at 400 W with 12.56 MHz, and the results of which are shown in Fig. 6 (b). Here, 20 mTorr of Ar/CF_4 (150/75 sccm) was used as the reactive gas mixture. As shown in Fig. 6(b), similar to the results observed in Figs. 5(b) and 6(a), the change in plasma density with increasing the RF power to the superimposed dual-frequency ICP source was generally higher for 13.56 MHz RF power compared to 2 MHz RF power. However, when the 13.56 MHz RF power was increased, the uniformity was degraded while, when the 2 MHz RF power was increased, the uniformity was similar or improved. In Fig. 7, one data point from Fig. 5(b) for the single-frequency ICP operation with only 800 W at 13.56 MHz, and one data point from Fig. 6(b) for the superimposed dual-frequency ICP operation with 800 W at 13.56 MHz and 1000 W at 2 MHz while biasing the substrate using 400 W at 12.56 MHz, are compared again. As shown in Fig. 7, by using the superimposed dual-frequency ICP for Ar/CF_4, similar to the results in Fig. 2 for Ar, improved plasma uniformity was obtained by increasing the plasma density at the center region of the wafer close to that of the edge region of the wafer.

A cartoon describing a possible mechanism for an improvement of the plasma uniformity using a superimposed dual-frequency ICP is shown in Fig. 8(a). As shown in Fig. 8(a), the complicated voltages are developed on the two-turn antenna line and these antenna voltages are transferred to the electrons in the plasma. That is, due to the formation of different voltages on different parts of the ICP antenna by using dual

frequency instead of single frequency, the electrons in the plasma tend to be accelerated to the radial direction (the electric field developed by capacitive coupling) in addition to the circumferential direction (the electric field direction developed by inductive coupling). The radial scattering of the electrons in the plasma tends to improve the plasma uniformity by distributing energetic electrons uniformly over the substrate surface. The complicated electric field to the electrons in the plasma promotes the electric field drift of electrons toward the radial direction of the wafer, and which can improve the plasma density as shown in Fig. 8(b). In addition, for the superimposed dual frequency ICP, the plasma density uniformity could be also improved by adding the plasma density profile by the 13.56 MHz RF power shown in Fig. 5 and that by the 2 MHz RF power shown in Fig. 6(a).

3.3. Etch results of superimposed dual-frequency ICP using Ar/CF_4

Using the results of the plasma characteristics obtained with the superimposed dual-frequency ICP source, actual SiO_2 coupon samples randomly distributed within a 300 mm diameter were etched, and the etch rates and etch uniformity were investigated in Fig. 9. Their results are shown in Fig. 9(a) and (b) for a single-frequency ICP operation with 800 W at 13.56 MHz and for a superimposed dual-frequency ICP operation with 800 W at 13.56 MHz and 1200 W at 2 MHz, respectively, while biasing the substrate with 400 W at 12.56 MHz. For each condition, 15 coupon samples of 2 cm × 2 cm SiO_2 on silicon were used, and the etch time was varied to etch a similar amount; therefore, for the single 800 W, 13.56 MHz ICP, the etch time was 4.5 min, whereas for the superimposed dual-frequency ICP operated with 800 W at 13.56 MHz and 1200 W at 2 MHz, the etch time was 3 min. As shown in Fig. 9(a) and (b), the total etch depth was ~300 nm for both conditions, although the non-uniformity of the etching was better (2.6%) for the superimposed dual-frequency ICP condition compared to that (3.9%) for the single-frequency ICP condition. Fig. 9(c) shows the etch rates of SiO_2 measured along the 300 mm diameter wafer centerline zone of A-A' in Fig. 9(a) and (b). As shown in Fig. 9(c), the etch uniformity change similar to the change of electron density uniformity shown in Fig. 2 could be observed, and which showed better etch uniformity for the superimposed ICP operation compared to the single frequency ICP operation by improving the etch rate at the wafer center region. In fact, even though the entire 300 mm wafer was not used during the SiO_2 etching, it is believed that a better etch uniformity could be obtained using a 300-mm diameter wafer for the superimposed dual-frequency ICP, as compared to a conventional single-frequency ICP.

4. Conclusions

In this study, the effects of a superimposed dual-frequency ICP operated at 13.56 MHz and 2 MHz on the plasma characteristics were investigated using Ar and Ar/CF_4, and the plasma characteristics were compared with those obtained using the ICP operated with a single frequency of only 13.56 or 2 MHz. The use of a superimposed dual-frequency ICP operated at 13.56 and 2 MHz improved the plasma uniformity compared to a single-frequency ICP operated at 13.56 or 2 MHz for both Ar and Ar/CF_4. When SiO_2 was etched using Ar/CF_4 while biasing the substrate with a separate RF power of 400 W at 12.56 MHz, similar to the plasma uniformity, the ICP operated using superimposed dual frequencies of 13.56 and 2 MHz showed a better etch uniformity compared to that operated with a single frequency of 13.56 MHz. It is believed that, even though a specific type of ICP antenna was used in this study for the superimposed dual frequency ICP, a similar effect can be expected in other ICP antenna types, and can contribute toward a further improvement in the plasma uniformity for other antenna types.

Acknowledgements

This research was supported by NRF-2016M3A7B4910429 and by a cooperative SEMES research project.

References

[1] K. Ishikawa, K. Karahashi, T. Ichiki, J.P. Chang, S.M. George, W.M.M. Kessels, H.J. Lee, S. Tinck, J.H. Um, K. Kinoshita, Progress and prospects in nanoscale dry processes: how can we control atomic layer reactions? Jpn. J. Appl. Phys. 56 (2017) 06HA02https://doi.org/10.7567/JJAP.56.06HA02.
[2] M.H. Khater, L.J. Overzet, A new inductively coupled plasma source design with improved azimuthal symmetry control, Plasma Sources Sci. Technol. 9 (2000) 545–561 https://doi.org/10.1088/0963-0252/9/4/310.
[3] M.A. Lieberman, A.J. Lichtenberg, Principles of Plasma Discharges and Materials Processing, second ed., Wiley, New York, 2005.
[4] S.H. Lee, J.H. Cho, S.R. Huh, G.H. Kim, Standing wave effect on plasma distribution in an inductively coupled plasma source with a short antenna, J. Phys. D Appl. Phys. 47 (2014) 015205https://doi.org/10.1088/0022-3727/47/1/015205.
[5] J.E. Stevens, M.J. Sowa, J.L. Cecchi, Uniformity of radio frequency bias voltages along conducting surfaces in a plasma, J. Vac. Sci. Technol. A 14 (1996) 139–143 https://doi.org/10.1116/1.579909.
[6] H.C. Lee, C.W. Chung, Impedance transition and series resonance between bulk plasma and sheath in biased inductively coupled plasma, Thin Solid Films 518 (2010) 5219–5222 https://doi.org/10.1016/j.tsf.2010.03.147.
[7] J. Robiche, P.C. Boyle, M.M. Turner, A.R. Ellingboe, Analytical model of a dual frequency capacitive sheath, J. Phys. D Appl. Phys. 36 (2003) 1810–1816 http://doi.org/10.1088/0022-3727/36/15/311.
[8] Q.H. Yuan, Y. Xin, G.Q. Yin, X.J. Huang, K. Sun, Z.Y. Ning, Effect of low-frequency power on dual-frequency capacitively coupled plasmas, J. Phys. D Appl. Phys. 41 (2008) 205209 https://doi.org/10.1088/0022-3727/41/20/205209.
[9] Y.X. Liu, Y.R. Zhang, A. Bogaerts, Y.N. Wang, Electromagnetic effects in high-frequency large-area capacitive discharges: a review, J. Vac. Sci. Technol. A 33 (2015) 020801https://doi.org/10.1116/1.4907926.
[10] H.C. Lee, S.J. Oh, C.W. Chung, Experimental observation of the skin effect on plasma uniformity in inductively coupled plasmas with a radio frequency bias, Plasma Sources Sci. Technol. 21 (2012) 035003https://doi.org/10.1088/0963-0252/21/3/035003.
[11] A. Perret, P. Chabert, J.-P. Booth, J. Jolly, J. Guillon, P. Auvray, Ion flux non-uniformities in large-area high-frequency capacitive discharges, Appl. Phys. Lett. 83 (2003) 243–245 https://doi.org/10.1063/1.1592617.
[12] D. Sung, V. Volynets, W. Hwang, Y. Sung, S. Lee, M. Choi, G.H. Kim, Frequency and electrode shape effects on etch rate uniformity in a dual-frequency capacitive reactor, J. Vac. Sci. Technol. A 30 (2012) 061301https://doi.org/10.1116/1.4754695.
[13] H.C. Lee, J.Y. Bang, C.W. Chung, Effects of RF bias power on electron energy distribution function and plasma uniformity in inductively coupled argon plasma, Thin Solid Films 519 (2011) 7009–7013 https://doi.org/10.1016/j.tsf.2011.01.218.
[14] A. Mishra, K.N. Kim, T.H. Kim, G.Y. Yeom, Synergetic effects in a discharge produced by a dual frequency-dual antenna large-area ICP source, Plasma Sources Sci. Technol. 21 (2012) 035018https://doi.org/10.1088/0963-0252/21/3/035018.
[15] Y.C. Kim, S.H. Jang, S.J. Oh, H.C. Lee, C.W. Chung, Two-dimensional-spatial distribution measurement of electron temperature and plasma density in low temperature plasmas, Rev. Sci. Instrum. 84 (2013) 053505https://doi.org/10.1063/1.4802673.
[16] W.H. Lee, H.W. Cheong, J.W. Kim, K.W. Whang, Improvement of uniformity in a weakly magnetized inductively coupled plasma, Plasma Sources Sci. Technol. 24 (2015) 065012https://doi.org/10.1088/0963-0252/24/6/065012.
[17] Y.X. Liu, F. Gao, J. Liu, Y.N. Wang, Experimental observation of standing wave effect in low-pressure very-high-frequency capacitive discharges, J. Appl. Phys. 116 (2014) 043303https://doi.org/10.1063/1.4891504.
[18] Y.R. Zhang, F. Gao, X.C. Li, A. Bogaerts, Y.N. Wang, Fluid simulation of the bias effect in inductive/capacitive discharges, J. Vac. Sci. Technol. A 33 (2015) 061303https://doi.org/10.1116/1.4928033.
[19] T. Denda, Y. Miyoshi, Y. Komukai, T. Goto, Z.Lj Petrović, T. Makabe, Functional separation in two frequency operation of an inductively coupled plasma, J. Appl. Phys. 95 (2004) 870–876 https://doi.org/10.1063/1.1636527.
[20] L. Sansonnens, J. Schmitt, Shaped electrode and lens for a uniform radio-frequency capacitive plasma, Appl. Phys. Lett. 82 (2003) 182–184 https://doi.org/10.1063/1.1534918.
[21] P. Chabert, J.-L. Raimbault, J.-L. Rax, A. Perrat, Suppression of the standing wave effect in high frequency capacitive discharges using a shaped electrode and a dielectric lens: self-consistent approach, Phys. Plasmas 11 (2004) 4081–4087 https://doi.org/10.1063/1.1770900.
[22] E. Monaghan, G.Y. Yeom, A.R. Ellingboe, Measurement of nc-Si:H film uniformity and diagnosis of plasma spatial structure produced by a very high frequency, differentially powered, multi-tile plasma source, Vacuum 119 (2015) 34–46 https://doi.org/10.1016/j.vacuum.2015.03.019.
[23] E. Monaghan, T. Michna, C. Gaman, D. O'Farrel, K. Ryan, D. Adley, T.S. Perova, B. Drews, M. Jaskot, A.R. Ellingboe, Characterisation of thin film silicon films deposited by plasma enhanced chemical vapour deposition at 162 MHz, using a large area, scalable, multi-tile-electrode plasma source, Thin Solid Films 519 (2011) 6884–6886 https://doi.org/10.1016/j.tsf.2011.04.092.
[24] E. Schungel, S. Mohr, J. Schulze, U. Czarnetzki, M.J. Kushner, Ion distribution

functions at the electrodes of capacitively coupled high-pressure hydrogen discharges, Plasma Sources Sci. Technol. 23 (2014) 015001https://doi.org/10.1088/0963-0252/23/1/015001.

[25] N. Sirse, A. Mishra, G.Y. Yeom, A.R. Ellingboe, Electron density modulation in pulsed dual-frequency (2/13.56MHz) dual-antenna inductively coupled plasma discharge, J. Vac. Sci. Technol. Vac., Surf. Films 34 (2016) 051302https://doi.org/10.1116/1.4959844.

[26] J. Brcka, Investigation of large-area multicoil inductively coupled plasma sources using three-dimensional fluid model, Jpn. J. Appl. Phys. 55 (2016) 07LD08https://doi.org/10.7567/jjap.55.07ld08.

[27] M.J. Kushner, Consequences of asymmetric pumping in low pressure plasma processing reactors: a three-dimensional modeling study, J. Appl. Phys. 82 (1997) 5312–5320 https://doi.org/10.1063/1.366297.

[28] P. Diomede, D.J. Economou, V.M. Donnelly, Particle-in-cell simulation of ion energy distributions on an electrode by applying tailored bias waveforms in the afterglow of a pulsed plasma, J. Appl. Phys. 109 (2011) 083302https://doi.org/10.1063/1.3573488.

[29] A. Mishra, J.S. Seo, K.N. Kim, G.Y. Yeom, Temporal evolution of plasma potential in a large-area pulsed dual-frequency inductively coupled discharge, J. Phys. D Appl. Phys. 46 (2013) 235203 https://doi.org/10.1088/0022-3727/46/23/235203.